PROCEEDINGS OF SCIENCE

Study of time-dependent and direct CP violation at Belle

Kazutaka Sumisawa[†a,*]

[a] *KEK,*
1-1 Oho, Tsukuba, Japan

E-mail: kazutaka.sumisawa@kek.jp

We present a new measurement of time-dependent CP violation in $B^0 \to K^0_S K^0_S K^0_S$, and direct CP violation in $B \to \overline{D^0}\pi$. These studies are based on the full Belle data set of $772 \times 10^6 B\overline{B}$ pairs collected at the $\Upsilon(4S)$ resonance.

40th International Conference on High Energy physics - ICHEP2020
July 28 - August 6, 2020
Prague, Czech Republic (virtual meeting)

[†] on behalf of the Belle Collaboration
[*] Speaker

PoS(ICHEP2020)429

1. Introduction

Study of CP violation provides test of the Standard Model (SM). In the SM, CP violation arises from the Kobayashi-Maskawa (KM) phase [1] in the quark-mixing matrix in the weak interaction. In particular, the SM predicts to a good approximation that $\mathcal{S} = -\xi_f \sin 2\phi_1$ and $\mathcal{A} = 0$ for both $b \to c\bar{c}s$ and $b \to s\bar{q}q$ transitions, where $\mathcal{S}$ ($\mathcal{A}$) is a parameter for mixing-induced (direct) CP violation [2], $\xi_f = +1(-1)$ corresponds to CP-even (-odd) final states and ϕ_1 is one of angles of the Unitarity Triangle. Measurements of time-dependent CP asymmetries in $B^0 \to J/\psi K^0_S$ and related decay modes, which are governed by the $b \to c\bar{c}s$ transition, by the Belle [3] and BaBar [4] collaborations already determine $\sin 2\phi_1$ rather precisely.

CP-violation parameters in the flavor-changing $b \to s$ transition are sensitive to phenomena at a very high-energy scale [5]. The B^0 decay to $K^0_S K^0_S K^0_S$, which is a $\xi_f = +1$ state, is one of the most promising modes for this purpose [6]. Since there is no u quark in the final state, the decay is dominated by the $b \to s\bar{s}s$ transition.

$B^0 \to \overline{D^0}\pi^0$ and $B^+ \to \overline{D^0}\pi^+$ decays are $b \to c\bar{u}d$ transitions. In these decays, the contribution of the higher level diagram is significantly lower than that of the tree level diagram. No A_{CP} is expected in SM. Both decays are commonly used as control modes in other analyses (for example, $B^0 \to \pi^0\pi^0$, $B \to K\pi$) and allow for high-precision validation of techniques. These analyses are therefore also important for Belle II precision frontier.

2. Belle detector

The Belle detector is a large-solid-angle magnetic spectrometer that consists of a silicon vertex detector (SVD), a 50-layer central drift chamber (CDC), an array of aerogel threshold Cherenkov counters (ACC), a barrel-like arrangement of time-of-flight scintillation counters (TOF), and an electromagnetic calorimeter comprised of CsI(Tl) crystals (ECL) located inside a superconducting solenoid coil that provides a 1.5 T magnetic field. An iron flux-return located outside the coil is instrumented to detect K^0_L mesons and to identify muons (KLM). The detector is described in detail elsewhere [7].

3. Measurement of time-dependent CP violation in $B \to K^0_S K^0_S K^0_S$

Signal candidates are identified by kinematic variables calculated using the information such as momentum, energy and particle identification from Belle detector. For the kinematic variables defined in the center of mass system (cms), the beam-energy constrained mass $M_{\rm bc} \equiv \sqrt{E^2_{\rm beam} - {p_B}^2}$ and the energy difference $\Delta E \equiv E_B - E_{\rm beam}$ are used, where $E_{\rm beam} = \sqrt{s}/2$ is the cms beam energy, and p_B and E_B are the cms three momentum and energy of the reconstructed B meson candidate, respectively. The dominant source of background is continuum $e^+e^- \to q\overline{q}$ ($q = u, d, s$, and c) production. To reduce it, a parameter, modified NN, is calculated using a neural network (NN) technique with a likelihood ratio from modified Fox-Wolfram moments [9], cosine of the angle between the beam direction and B^0 flight derection, and the angle between the thrust axis of the B^0 candidate and that of the rest of the event. The event selection and extraction of CP violation are optimized using Monte Carlo (MC) simulated events. The MC events are generated

by EVTGEN [10] and the detector response is modeled using GEANT3 [11]. For signal extraction, we used an unbinned maximum likelihood fit with 3D probability density function (PDF) (ΔE, $M_{\rm bc}$, and modified NN), as shown in Fig.1. Obtained are 329 ± 20 signal events, with 72% purity in the signal region.

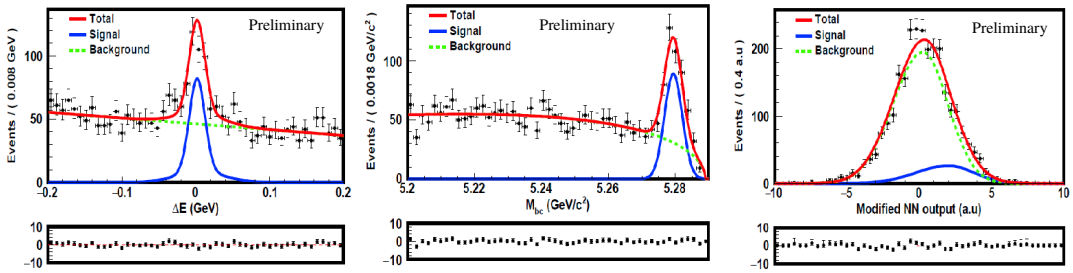

Figure 1: Fit projections from the signal extracion obtained using three-dimensional fit to ΔE (left), $M_{\rm bc}$ (middle), and modified NN (right) distributions.

In the decay chain $\Upsilon(4S) \to B^0\overline{B^0} \to f_{CP} f_{\rm tag}$, where one of the B mesons decays at time t_{CP} to a CP eigenstate f_{CP} and the other decays at time $t_{\rm tag}$ to a final state $f_{\rm tag}$ that distinguishes between B^0 and $\overline{B^0}$, the decay rate has a time dependence given by

$$\mathcal{P}(\Delta t) = \frac{e^{-|\Delta t|/\tau_{B^0}}}{4\tau_{B^0}} \left\{ 1 + q \cdot \Big[\mathcal{S} \sin(\Delta m \Delta t) + \mathcal{A} \cos(\Delta m \Delta t) \Big] \right\}. \tag{1}$$

Here τ_{B^0} is the B^0 lifetime, Δm is the mass difference between the two B^0 mass eigenstates, Δt is the time difference $t_{CP} - t_{\rm tag}$, and the b-flavor charge is $q = +1$ (-1) when the tagging B meson is a B^0 ($\overline{B^0}$).

The b-flavor of the accompanying B meson is identified from inclusive properties of particles that are not associated with the reconstructed $B^0 \to K^0_S K^0_S K^0_S$ candidates. The algorithm for flavor tagging is described in detail elsewhere [12]. We use two parameters, q defined in Eq. (1) and r, to represent the tagging information. The parameter r is an event-by-event, MC-determined flavor-tagging dilution factor that ranges from $r = 0$ for no flavor discrimination to $r = 1$ for unambiguous flavor assignment. Candidates with $r \leq 0.1$ are not used for CP violation measurement. The remaining data are sorted into six r intervals. The wrong tag fractions w for each of the r intervals and their differences Δw for B^0 and $\overline{B^0}$ decays are determined from B^0 decay control sample in which the flavor is specified by itself.

We determine $\mathcal{S}$ and $\mathcal{A}$ by performing an unbinned maximum-likelihood fit to the observed Δt distribution. The PDF expected for the signal distribution, $\mathcal{P}_{\rm sig}(\Delta t; \mathcal{S}, \mathcal{A}, q, w, \Delta w)$, is given by Eq. (1) after incorporating the effect of incorrect flavor assignment. The distribution is convolved with the proper-time interval resolution function, which is a function of event-by-event B-vertex errors. We determine the following likelihood value for each event i:

$$P_i = (1 - f_{\rm ol}) \Big[f_{\rm sig} \mathcal{P}_{\rm sig}(\Delta t_i) + (1 - f_{\rm sig}) \mathcal{P}_{\rm bkg}(\Delta t_i) \Big] + f_{\rm ol} \mathcal{P}_{\rm ol}(\Delta t_i), \tag{2}$$

where $\mathcal{P}_{\rm ol}$ is a broad Gaussian function that represents an outlier component with a small fraction $f_{\rm ol}$. The signal probability $f_{\rm sig}$ is calculated on an event-by-event basis from the function obtained

by the fit used to extract the signal yield. $\mathcal{P}_{\rm bkg}$ is PDF for background events, and it is determined by the fit to the Δt distribution of a background-enhanced control sample, i.e. events outside of the ΔE-$M_{\rm bc}$ signal region. We fix τ_{B^0} and Δm to their world-average values [13]. In order to reduce the statistical error on $\mathcal{A}$, we include events without B-vertex information. The likelihood value in this case is obtained from the function of Eq. (2) integrated over Δt_i.

The only free parameters in the final fit are $\mathcal{S}$ and $\mathcal{A}$, which are determined by maximizing the likelihood function $L = \prod_i P_i(\Delta t_i; \mathcal{S}, \mathcal{A})$ where the product runs over all events. Using the fit,

$$\mathcal{S} = -0.72 \pm 0.23(\text{stat}) \pm 0.05(\text{syst}), \ \mathcal{A} = 0.11 \pm 0.16(\text{stat}) \pm 0.05(\text{syst}) \tag{3}$$

are obtained [14]. The Δt and asymmetry distributions are shown in Fig. 2. Using the Feldman-Cousins approach [15], the significance of CP violation is obtained to be 2.4σ from the 2-dimenstional confidence region is the $\mathcal{S}$ and $\mathcal{A}$ plane, and is shown in Fig. 3.

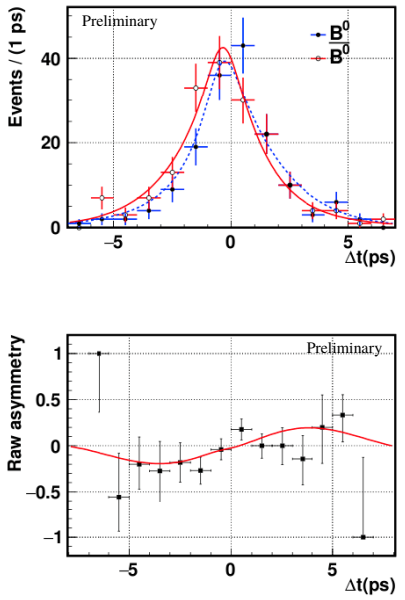

Figure 2: Δt distribution (top) and asymmetry distribution (bottom) obtained from data.

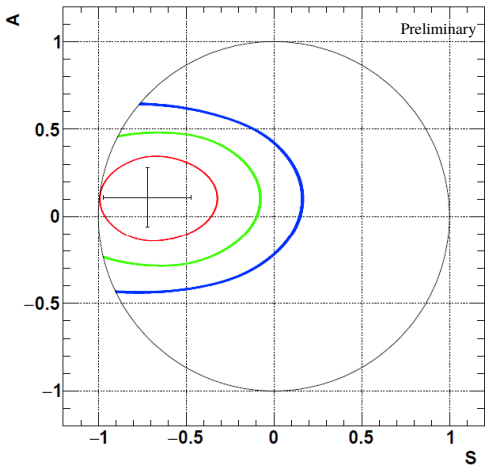

Figure 3: Confidence region for $\mathcal{S}$ and $\mathcal{A}$. The red, green, and blue contours represent 1σ, 2σ, and 3σ, respectively. The point with error bars represents the measured values. The circle is a physical region defined by $\mathcal{S}^2 + \mathcal{A}^2 \leq 1$.

4. Direct CP violation in $B \to \overline{D^0}\pi$

We reconstruct $B \to \overline{D^0}\pi$ candidates from the subsequent decays of the $\overline{D^0}$ and reconstructed $\pi^\pm$ or π^0 candidates. We employ two reconstruction modes: $B \to (\overline{D^0} \to K^+\pi^-)\pi$ (B_{2b}) and $B \to (\overline{D^0} \to K^+\pi^-\pi^0)\pi$ (B_{3b}). The π^0 mesons are reconstructed from their decay into two photons.

The direct CP violation parameter, A_{CP}, for the $B^0 \to \overline{D^0}\pi^0$ decay is defined as:

$$A_{CP} = \frac{\Gamma(\overline{B^0} \to D^0\pi^0) - \Gamma(B^0 \to \overline{D^0}\pi^0)}{\Gamma(\overline{B^0} \to D^0\pi^0) + \Gamma(B^0 \to \overline{D^0}\pi^0)}, \tag{4}$$

where Γ is the partial decay width for the corresponding decay.

Two kinematic variables, ΔE and $M_{\rm bc}$, and one variable for continuum suppresion, C'_{NN}, are used for extraction of signal yield and A_{CP}. Branching fraction ($\mathcal{B}$) and A_{CP} were determined via a simultaneous fit to subsequent 4 data sets (2 B-flavor and 2 D^0-decay modes (B_{2b} or B_{3b})).

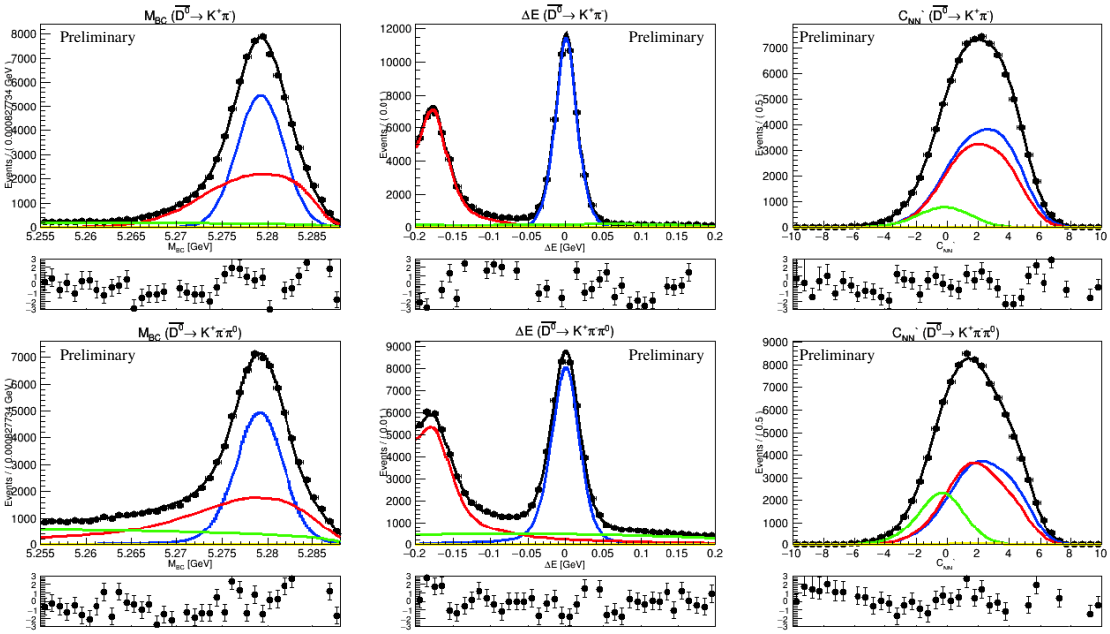

Figure 4: Projections of the $B^+ \to \overline{D^0}\pi^+$ fit result into the signal region for $M_{\rm bc}$ (left), ΔE (middle), and C'_{NN} (right) split into B_{2b} mode (top) and B_{3b} (bottom). The blue line shows signal PDF, red shows $B\overline{B}$ background PDF, green shows continuum background PDF, yellow shows rare background PDF, black is sum of all PDFs, and point are data.

To validate the reconstruction efficiencies and fitting methodology, we use the same techniques to analyze a control mode, $B^+ \to \overline{D^0}\pi^+$, resulting in $\mathcal{B} = (4.53 \pm 0.02 \pm 0.14) \times 10^3$ and $A_{CP} = (0.19 \pm 0.36 \pm 0.57)\%$, where the uncertainties quoted are statistical and systematic respectively. The obtained values are consistent with the PDF average values [13]. Fit results are shown in Fig. 4.

After fixing analysis procedures from the study of the control mode, we fit the $B^0 \to \overline{D^0}\pi^0$ decay mode data. The results are

$$\mathcal{B} = (2.69 \pm 0.06 \pm 0.09) \times 10^4, \; A_{CP} = (0.10 \pm 2.05 \pm 1.22)\%, \tag{5}$$

where the quoted uncertainies are statistical and systematic, respectively. Fit results are shown in Fig. 5. Our measurement of A_{CP} is the first result for this mode. It is consistent with the theoretically expected value of zero.

References

[1] M. Kobayashi and T. Maskawa, Prog. Theor. Phys. **49**, 652 (1973).

[2] A. B. Carter and A. I. Sanda, Phys. Rev. D **23**, 1567 (1981); I. I. Bigi and A. I. Sanda, Nucl. Phys. **B193**, 85 (1981).

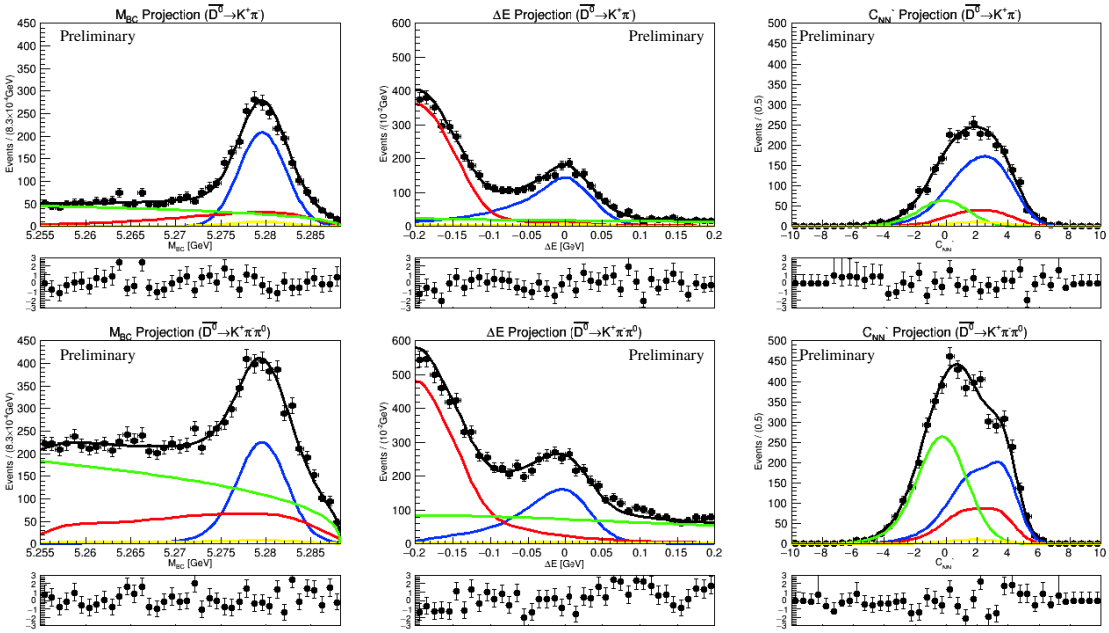

Figure 5: Projections of the $B^0 \to \overline{D}^0\pi^0$ fit result into the signal region for $M_{\rm bc}$ (left), ΔE (middle), and C'_{NN} (right) split into B_{2b} mode (top) and B_{3b} (bottom). The blue line shows signal PDF, red shows $B\overline{B}$ background PDF, green shows continuum background PDF, yellow shows rare background PDF, black is sum of all PDFs, and point are data.

[3] K. Abe *et al.* (Belle Collab.), Phys. Rev. Lett. **87**, 091802 (2001); Phys. Rev. D **66**, 032007 (2002); Phys. Rev. D **66**, 071102 (2002).

[4] B. Aubert *et al.* (Babar Collab.), Phys. Rev. Lett. **89**, 201802 (2002); hep-ex/0408127.

[5] Y. Grossman and M. P. Worah, Phys. Lett. B **395**, 241 (1997).

[6] T. Gershon and M. Hazumi, Phys. Lett. B **596**, 163 (2004).

[7] A. Abashian *et al.* (Belle Collab.), Nucl. Instr. and Meth. A **479**, 117 (2002).

[8] Z. Natkaniec *et al.* (Belle SVD2 Group), Nucl. Instr. and Meth. A **560**, 1 (2006).

[9] S. H. Lee *et al.* (Belle Collab.), Phys. Rev. Lett. **91**, 261801 (2003).

[10] D. J. Lange *et al.*, Nucl. Instr. and Meth. A **462**, 152 (2001).

[11] R. Brun *et al.*, GEANT 3.21, Report No. CERN DD/EE/84-1 (1984).

[12] H. Kakuno *et al.*, Nucl. Instr. and Meth. A **533**, 516 (2004).

[13] M. Tanabashi *et al.* (Particle Data Group), Phys. Rev. D **98**, 030001 (2018).

[14] The updated result is submitted as arXiv:2011.00793.

[15] G. J. Feldman and R. D. Cousins, Phys. Rev. D **57**, 3873 (1998).